

## Supporting Information

### Glass transition and dynamics of semiflexible polymer brushes

Jian-Hua Huang\*, Dan-Dan Sun, Rong-Xing Lu

*Department of Chemistry, Key Laboratory of Surface & Interface Science of Polymer Materials of Zhejiang Province, Zhejiang Sci-Tech University, Hangzhou 310018, China.*

Corresponding Author

\* Jian-Hua Huang (jhhuang@zstu.edu.cn)

#### 1. Influence of cooling rate

We have simulated the glass transition with three constant cooling rates  $1 \times 10^{-4}$ ,  $1 \times 10^{-5}$  and  $1 \times 10^{-6}$   $[(\epsilon/k_B)/\tau_0]$  for polymer brushes, respectively. Fig. S1a shows the dependence of the brush height  $h$  on temperature  $T$  for the three cooling rates for flexible ( $k_\theta = 0$ ) polymer brush. We find that, except the high cooling rate case ( $1 \times 10^{-4}$ ), there is no obvious difference for low cooling rate cases with  $1 \times 10^{-5}$  and  $1 \times 10^{-6}$ . A slightly higher  $T_g$  in the high cooling rate case is consistent with theory. Our results show that  $T_g$  is roughly independent of the cooling rate when the cooling rate is smaller than  $1 \times 10^{-5}$   $[(\epsilon/k_B)/\tau_0]$ .

Fig. S1b shows the dependence of mean square radius of gyration  $\langle R_g^2 \rangle$  of polymer chains on temperature  $T$  for three cooling rates for flexible ( $k_\theta = 0$ ) polymer brush. We also find that  $\langle R_g^2 \rangle$  is roughly the same for the cooling rates of  $1 \times 10^{-5}$  and  $1 \times 10^{-6}$   $[(\epsilon/k_B)/\tau_0]$ .

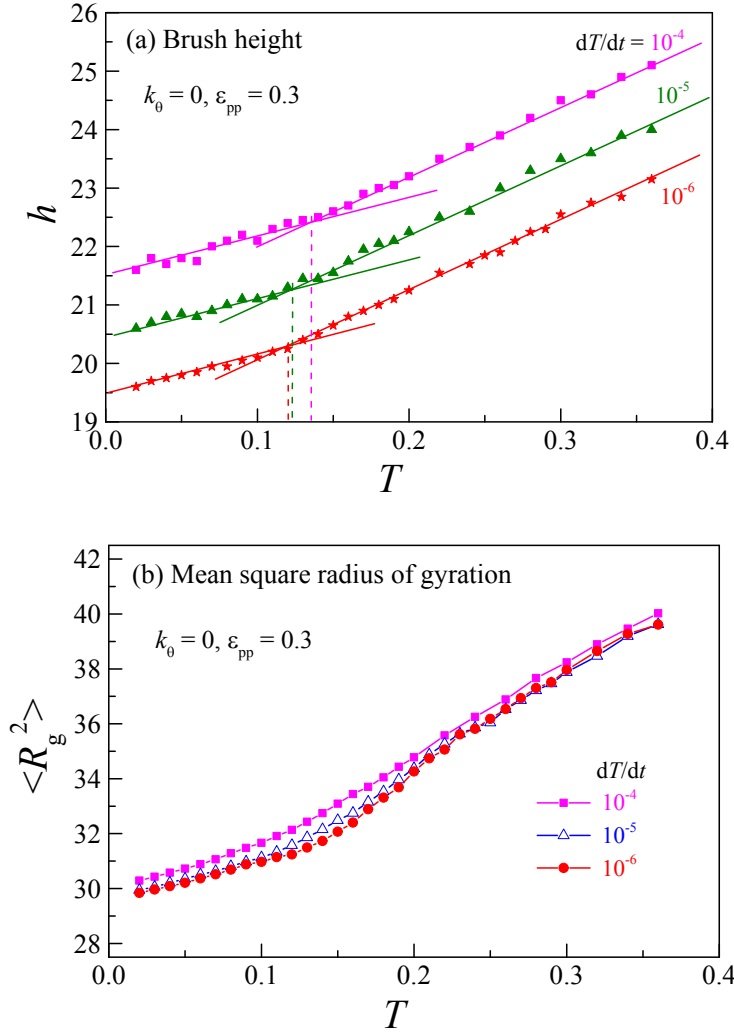


**Fig. S1** Plot of the brush height  $h$  (a) and mean square radius of gyration  $\langle R_g^2 \rangle$  (b) of flexible ( $k_0 = 0$ ) polymer brushes versus temperature  $T$  for different cooling rates:  $dT/dt = 10^{-4}$ ,  $10^{-5}$ , and  $10^{-6}$ . The glass transition temperature  $T_g$  is indicated by dashed lines. For clarification,  $h$  of  $dT/dt = 10^{-4}$  is shifted by 2, and that of  $dT/dt = 10^{-5}$  is shifted by 1.

## 2. Persistence length

Fig. S2 presents the persistence length  $L_p$  for semi-flexible polymer in solution at temperature  $T = 1$ . We find that  $L_p$  increases linearly with the bending modulus  $k_0$ . The inset of Fig. S2 shows that  $L_p$  decreases with increasing  $T$  as  $L_p = L_p(1)/T$ .

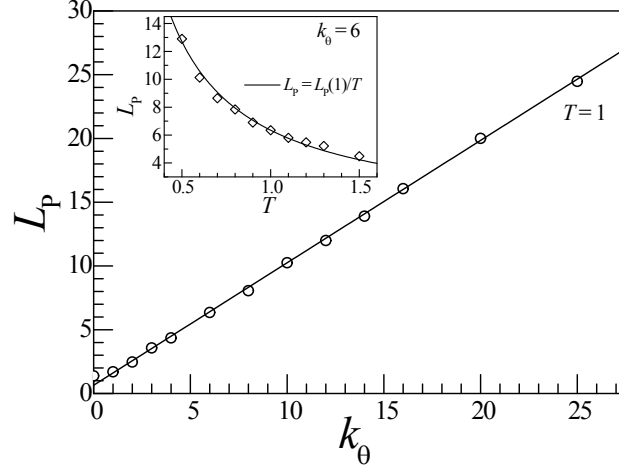


**Fig. S2** Plot of persistence length  $L_p$  versus bending modulus  $k_\theta$  for the semi-flexible polymer in solution at  $T = 1$ . The inset shows the dependence of  $L_p$  on  $T$  for  $k_\theta = 6$ .  $L_p(1)$  denotes  $L_p$  at  $T = 1$ .

### 3. Size effect

We have examined the tilt of polymer chains in the semiflexible polymer brush with  $k_\theta = 6$  in a larger system with  $L_x = L_y = 40$ . Fig. S3 shows the mean square end-to-end distance  $\langle R^2 \rangle$  and mean tilt angle  $\langle \phi \rangle$  for systems with  $L_x = L_y = 30$  and 40. We find the size effect can be neglected.

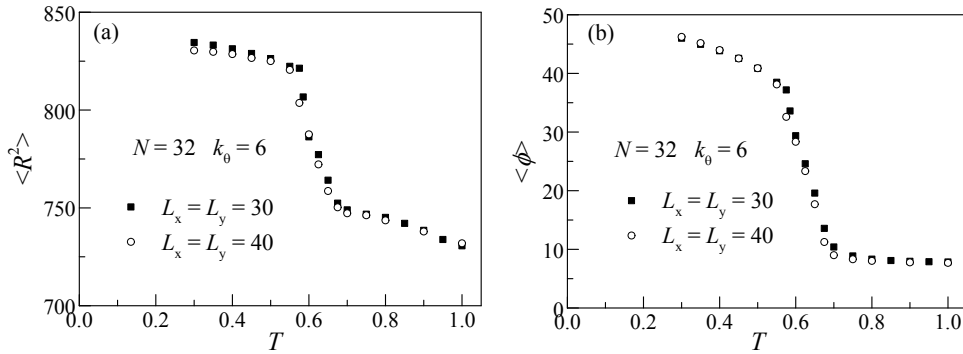


**Fig. S3** Variation of (a) mean-square end-to-end distance  $\langle R^2 \rangle$  and (b) mean tilt angle  $\langle \phi \rangle$  of polymer chains with  $N = 32$  and  $k_\theta = 6$  in the  $30 \times 30 \times 50$  and  $40 \times 40 \times 50$  systems.

### 4. lateral position fluctuation

Fig. S4 presents the lateral position fluctuation  $\sigma_{||}^2$  for the fully flexible ( $k_\theta = 0$ ) and semiflexible ( $k_\theta = 6$ ) polymer brushes at temperature slightly higher than  $T_g$ . We can see the free-surface effect with large  $\sigma_{||}^2$  for large segment indexes and the

substrate effect with small  $\sigma_{\parallel}^2$  for small segment indexes.

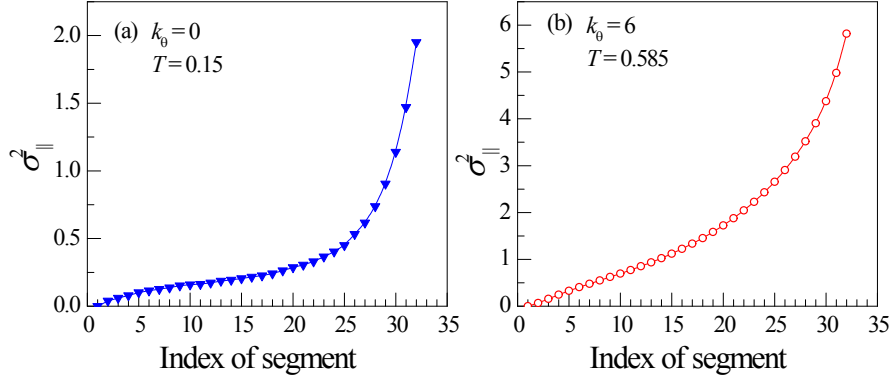


**Fig. S4** Profile of the lateral position fluctuation  $\sigma_{\parallel}^2$  for the fully flexible ( $k_{\theta} = 0$ ) and semiflexible ( $k_{\theta} = 6$ ) polymer brushes. Temperature is a little higher than  $T_g$ . Polymer length  $N = 32$ .

## 5. Autocorrelation function of bond vectors

The autocorrelation function of a bond vector is defined as

$$\rho_b(t) = \frac{\langle \vec{b}(t) \cdot \vec{b}(0) \rangle}{\langle b^2 \rangle} \quad (1)$$

with  $\vec{b}(0)$  and  $\vec{b}(t)$  the bond vector at time  $t = 0$  and  $t$ , respectively. The bracket denotes an average over chains and independent samples.

Fig. S5(a) presents the evolution of  $\rho_b(t)$  for the 15th and 31st bonds in the polymer chains for flexible ( $k_{\theta} = 0$ ) and semiflexible ( $k_{\theta} = 6$ ) polymer brushes. Polymer length is  $N = 32$ . The 15th and 31st bonds correspond to the middle and tail bonds, respectively. We find  $\rho_b(t)$  decreases with time. However, it does not decay to 0 even at long time, except that close to the free end of the flexible polymer chains. For the semiflexible polymer brush with  $k_{\theta} = 6$ , the decay of  $\rho_b(t)$  is very limited due to the chain rigidity. Therefore, we are not able to estimate the relaxation time from the  $1/e$  value. Moreover, we also find that the decrease of  $\rho_b(t)$  does not obey a single exponent decay.<sup>1,2</sup> On the contrary, the exponent is of time dependence as shown in Fig. S5(b). Therefore, we are not able to estimate the relaxation time from the exponent decay of  $\rho_b(t)$ , and in consequence we are not able to calculate the local glass transition temperature in the polymer brush. Our results indicate that the

dynamics of polymer brushes is different from that of polymer films (floating on substrate). It was pointed out that the local glass transition temperature could be obtained based on the autocorrelation function for polymer films.<sup>3</sup>

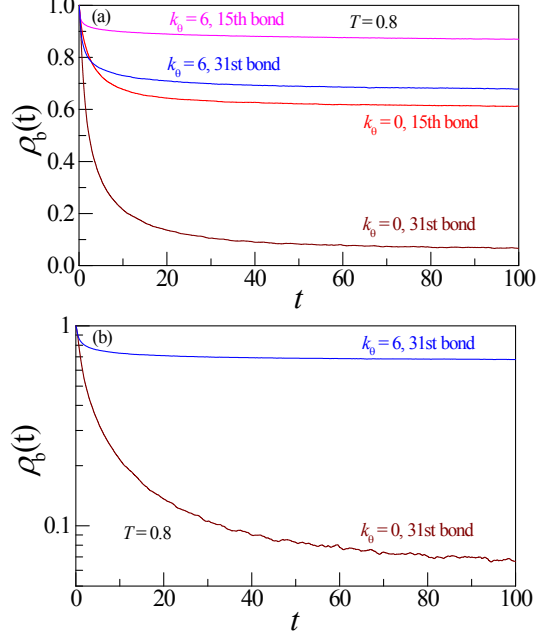


**Fig. S5** Linear plot (a) and semi-logarithm plot (b) for the evolution of the autocorrelation function  $\rho_b(t)$  of the 15th and 31st bond in flexible ( $k_\theta = 0$ ) and semiflexible ( $k_\theta = 6$ ) polymer brushes. Polymer length  $N = 32$ , temperature  $T = 0.8$ .

## 6. Mean square displacement of segments

The lateral mean square displacement (MSD) of a segment is defined as

$$\langle \Delta r^2 \rangle_{||}(t) = \langle [x(t) - x(0)]^2 + [y(t) - y(0)]^2 \rangle \quad (2)$$

with  $x(t)$ ,  $y(t)$  the lateral position of the segment at time  $t$ . The lateral MSD is averaged over all segments of the same index and over all independent samples. The lateral MSDs are calculated for segment indexes from 2 to  $N$ .

Fig. S6 presents the evolution of the lateral MSD of the 16th and 32nd segments with time in the flexible ( $k_\theta = 0$ ) and semiflexible ( $k_\theta = 6$ ) polymer brushes at  $T = 0.8$ . Different from that in polymer melts or in polymer films, the MSD of individual segments in polymer brushes increases with time and finally saturates at a plateau value,<sup>1</sup> we thus can't obtain the diffusion coefficient as in bulk or in films. Compared with the flexible polymer brush, the semiflexible one needs much longer time to reach

the plateau. And the lower the temperature is, the longer time is needed to reach the plateau value. Therefore, it is difficult to obtain the final plateau value without running too long time at low temperature especially close to  $T_g$ . Some groups arbitrarily defined a relaxation time  $\tau$ , at which the lateral MSD has reached 2/3 or 3/4 of its final saturation value,<sup>1</sup> or a segment's distance,<sup>4</sup> to characterize the dynamics of polymer brushes.

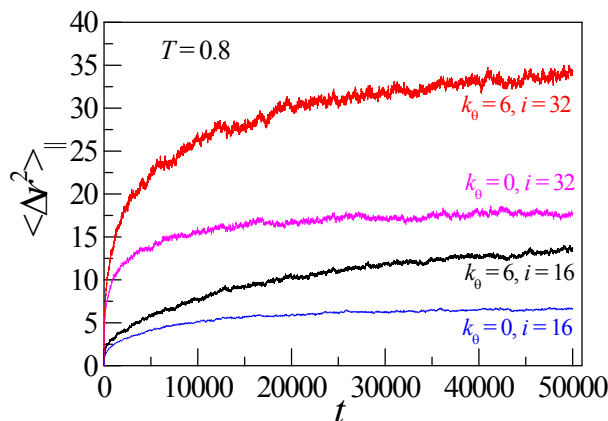


**Fig. S6** Evolution of the lateral MSD,  $\langle \Delta r^2 \rangle_{\parallel}$ , of the 16th and 32nd segments with time in flexible ( $k_{\theta} = 0$ ) and semiflexible ( $k_{\theta} = 6$ ) polymer brushes at  $T = 0.8$ .

We have recorded the lateral MSD of individual segments at different simulation times and temperatures. Fig. S7 present the dependence of the lateral MSD of the tail segment ( $i = 32$ ) on the temperature  $T$  for the fully flexible ( $k_{\theta} = 0$ ) and semiflexible ( $k_{\theta} = 6$ ) polymer brushes at  $t = 50000$  (in unit of  $\tau_0$ ). We find the lateral MSD roughly tends to 0 at low temperature. As shown in Fig. S7, the local glass transition temperature,  $T_{g,local}$ , is estimated as the temperature at which the two straight lines representing the movable and frozen regions, respectively, intersect with each other.

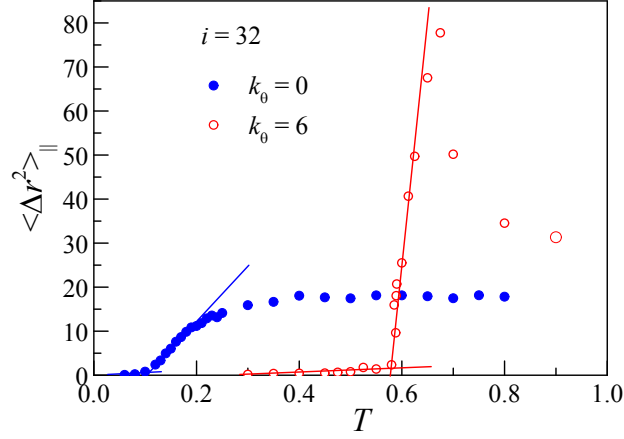


**Fig. S7** Variation of the lateral MSD,  $\langle \Delta r^2 \rangle_{\parallel}$ , of the tail segment ( $i = 32$ ) with temperature  $T$  for the fully flexible ( $k_{\theta} = 0$ ) and semiflexible ( $k_{\theta} = 6$ ) polymer brushes after running for 50000 at each temperature.

We have estimated  $T_{g,local}$  from the lateral MSD at different simulation times. We find that  $T_{g,local}$  is dependent on the simulation time as shown in Fig. S8, especially for the fully flexible polymer brush. As the simulation time increases,  $T_{g,local}$  tends to the pseudo-thermodynamical glass transition temperature,  $T_g$ , determined from the temperature-dependent brush height. The result indicates that a longer time is better to estimate  $T_{g,local}$ . However, for the semiflexible ( $k_{\theta} = 6$ ) polymer brush, the value of  $T_{g,local}$  is of less time dependence.

The decrease of  $T_{g,local}$  with segment index shown in Fig. S8 is resulted from the confinement effect of substrate, similar to that determined from the lateral fluctuation of segments.

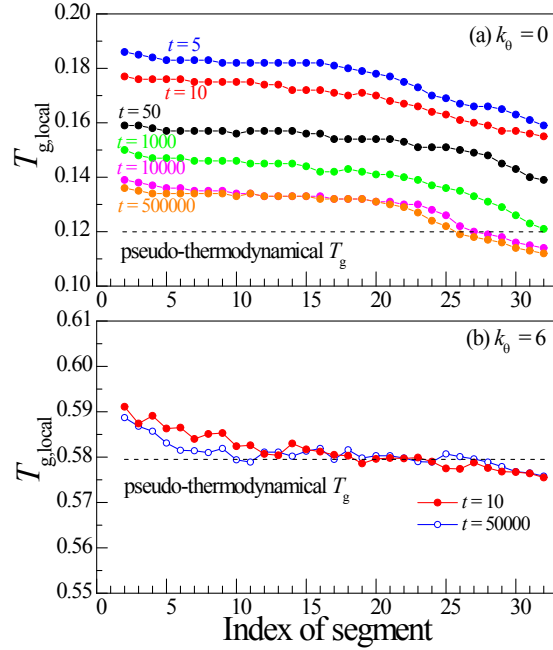


**Fig. S8** Local glass transition temperature ( $T_{g,local}$ ) of individual segments in the fully flexible ( $k_0 = 0$ ) and semiflexible ( $k_0 = 6$ ) polymer brush estimated based on the variation of lateral MSD at different times in annealing process. The dash lines indicate the corresponding pseudo-thermodynamical glass transition temperature  $T_g$  estimated from the temperature-dependent brush height.

## 7. Random grafted polymer brushes

We have also simulated the variation of brush height with temperature and  $T_{g,local}$  of individual segments for fully flexible ( $k_0 = 0$ ) and semiflexible ( $k_0 = 6$ ) polymer brushes which are randomly grafted (but without overlap) on the substrate. The results are presented in Fig. S9. It is found that  $T_g$  and  $T_{g,local}$  of randomly grafted polymer brushes are roughly the same as that of regularly grafted ones.

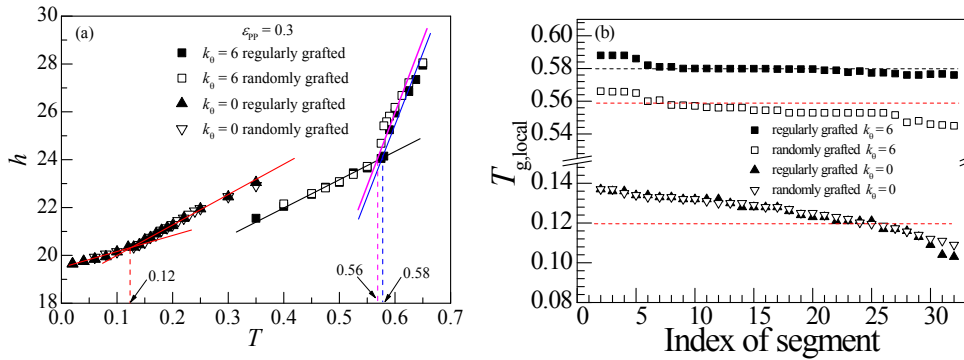


**Fig. S9** Comparison of the temperature dependence of the brush height  $h$  (a) and the local glass transition temperature  $T_{g,local}$  of individual segments determined from the

temperature-dependent lateral position fluctuation  $\sigma_{\parallel}^2$  (b) for the flexible ( $k_{\theta} = 0$ ) and semiflexible ( $k_{\theta} = 6$ ) polymer brushes grafted randomly and regularly on the substrate, respectively. The dash line in (b) presents the corresponding value of  $T_g$ .

### References:

- [1] D. Reith, A. Milchev, P. Virnau and K. Binder, Computer simulation studies of chain dynamics in polymer brushes. *Macromolecules*, 2012, **45**, 4381–4393.
- [2] M. Lang, M. Werner, R. Dockhorn and T. Kreer, Arm retraction dynamics in dense polymer brushes. *Macromolecules*, 2016, **49**, 5190–5201.
- [3] C. Batistakis, A. V. Lyulin and M. A. J. Michels, Slowing down versus acceleration in the dynamics of confined polymer films. *Macromolecules*, 2012, **45**, 7282–7292.
- [4] S. -J. Xie, H. -J. Qian and Z. -Y. Lu, Polymer brushes: A controllable system with adjustable glass transition temperature of fragile glass formers. *J. Chem. Phys.*, 2014, **140**, 044901.